VISCOUS FLOW CALCULATIONS FOR THE AGARD STANDARD CONFIGURATION AIRFOILS WITH EXPERIMENTAL COMPARISONS

JAMES T. HOWLETT
UNSTEADY AERODYNAMICS BRANCH
NASA LANGLEY RESEARCH CENTER

This paper reports on recent experience in calculating unsteady transonic flows by means of viscous-inviscid interactions with the XTRAN2L computer code (ref. 1). The boundary-layer method for attached flows is based upon the work of Rizzetta (ref. 2) as implemented in reference 3. The non-isentropic corrections of Fuglsang and Williams (ref. 4) have also been incorporated along with the viscous interaction for some cases and initial results are presented. For unsteady separated flows, the inverse boundary-layer equations developed by Vatsa and Carter in reference 5 are used in a quasi-steady manner and preliminary results are presented. Currently, efforts are underway to include the viscous interactions in 3-D calculations in a stripwise fashion although no results for the 3-D work are presented herein.

UNSTEADY TRANSONIC VISCOUS-INVISCID INTERACTIONS

- ATTACHED FLOW (ARC, RIZZETTA)
  - THEORY WELL-DEVELOPED
  - EXTENSIVE APPLICATIONS
- NONISENTROPIC CORRECTIONS WITH VISCOUS EFFECTS
  - INITIAL THEORY
  - LIMITED APPLICATIONS
- SEPARATED FLOW
  - PRELIMINARY THEORY
  - LIMITED APPLICATIONS
- 3-D FLOW
  - XTRAN3
  - CAP-TSD

The inviscid code used in this study is the XTRAN2L computer code described in reference 1. The viscous boundary layer analysis is based upon Green's lag-entrainment equations as described in reference 2. For attached flow, the equations are used in the direct form: pressure from the inviscid analysis is specified and the equations are integrated to obtain the boundary-layer displacement thickness δ^*. For separated flows, the equations are inverted as described in reference 5 and the mass flow $\bar{m}$ is specified as input. In the inverse method, the boundary-layer displacement thickness δ^* is updated using Carter's method (ref. 6). For both the direct and the inverse method, the effect of the viscous boundary layer is included in the inviscid analysis by means of the airfoil surface tangency boundary condition.

BOUNDARY LAYER ANALYSIS

DIRECT

$$\begin{Bmatrix} \theta \\ \bar{H} \end{Bmatrix}_x = \{A_1\} + \{A_2\}\,\phi_{xx}$$

INVERSE

$$\begin{Bmatrix} \phi_x \\ \bar{H} \end{Bmatrix}_x = \{A_3\} + \{A_4\}\,\bar{m}_x$$

$$\bar{m} = \rho u \delta^*$$

$$(C_E)_x = A_5 + A_6\,\phi_{xx}$$

$$\delta^{*n+1} = H^n \theta^n$$

$$\delta^{*n+1} = \delta^{*n} + \omega \delta^{*n} \left(\frac{u_v}{u_I} - 1\right) \text{ (CARTER)}$$

AIRFOIL BOUNDARY CONDITION

$$\phi_y = F_x + F_t + \delta^*_x$$

Non-isentropic modifications to the transonic small disturbance (TSD) equation were developed by Fuglsang and Williams in reference 4. These modifications include a streamwise flux that satisfies the Prandtl relations at shock jumps, convection of shock generated entropy in the wake, and an entropy correction in the pressure coefficient. The non-isentropic modifications have been incorporated into the computer code along with the viscous-inviscid interactions and some initial calculations are presented.

NONISENTROPIC MODIFICATIONS TO TSD EQUATION (FUGLSANG AND WILLIAMS)

- MODIFIED STREAMWISE FLUX SATISFYING PRANDTL RELATION AT SHOCK JUMPS
- CONVECTION OF SHOCK GENERATED ENTROPY IN WAKE
- ENTROPY CORRECTION IN PRESSURE COEFFICIENT

This figure illustrates one of the numerical difficulities encountered with the interacting boundary-layer calculation. The original version of the computer code included an upwind switch in the evaluation of the pressure gradient term ϕ_{xx} for input to the boundary-layer equations. This upwind switch introduced a discontinuity in the unsteady forces when the shock moved across a grid point. The dashed line in the figure shows this discontinuity in the moment coefficient for a typical case. The purpose of upwind switching in computational fluid dynamics is to account properly for the domain of dependence in the numerical solution of partial differential equations. However, the present application merely requires numerically computing the derivative of a known function. Hence, upwind switching is not required. The solid line in the figure shows that the moment coefficient varies smoothly in time when upwind switching is not used. For all results presented in this paper, upwind switching is not used in the boundary-layer calculation. However, the inviscid solution algorithm does use upwind switching in the standard manner.

EFFECT OF UPWIND SWITCH IN BOUNDARY LAYER CALCULATION

NACA 64A010A **M = 0.796**

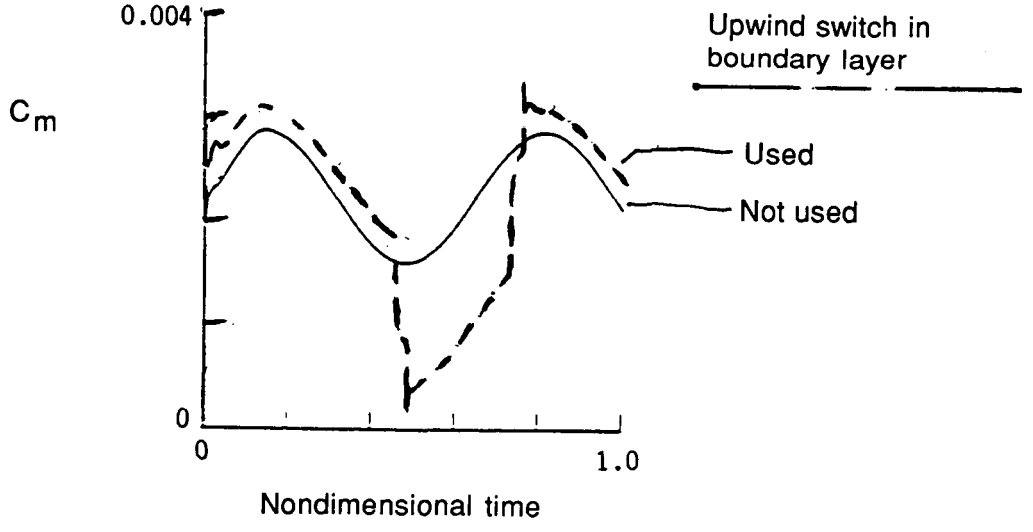

This figure shows steady pressure distributions for the NACA 64A006 airfoil for a range of Mach numbers. For the subsonic cases, the viscous and inviscid results are nearly identical except for small differences near the trailing edge where the viscous results more closely match the experiment. At M = 0.850, a shock wave develops near midchord and the viscous calculation agrees much better with the experiment than the inviscid result. For M = 0.875, the shock strengthens and moves aft. In this case, both the viscous and inviscid calculations exhibit differences from the experiment although the viscous result is closer to the experiment in the vicinity of the shock. Downstream of the shock the viscous result is in good agreement with the experiment.

STEADY PRESSURE DISTRIBUTION FOR NACA 64A006 AIRFOIL

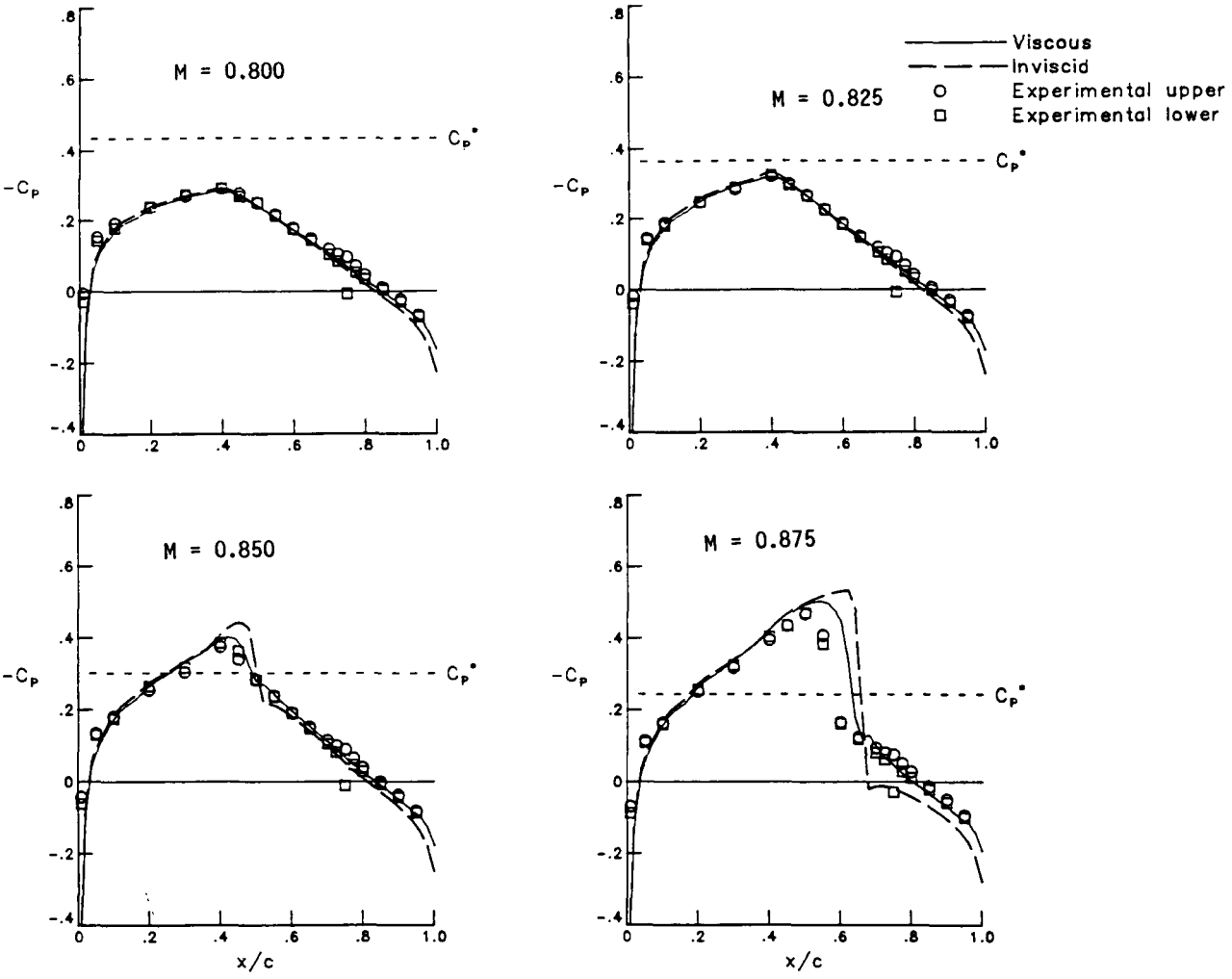

This figure shows plots of the boundary-layer displacement thickness for several mach numbers for steady calculations for the NACA 64A006 airfoil. For the two lowest values of Mach number, the results are subcritical and the displacement thickness increases smoothly in the downstream direction as Mach number is increased. At M = 0.850, the displacement thickness shows a slight increase due to the shock wave near midchord. For M = 0.875, the calculated result has a strong shock near 60% chord and the displacement thickness increases significantly across this shock. A further increase in Mach number to 0.960 moves the shock off the trailing edge and the displacement thickness increases slowly as the trailing edge is approached.

EFFECT OF MACH NUMBER ON DISPLACEMENT THICKNESS FOR NACA 64A006 AIRFOIL

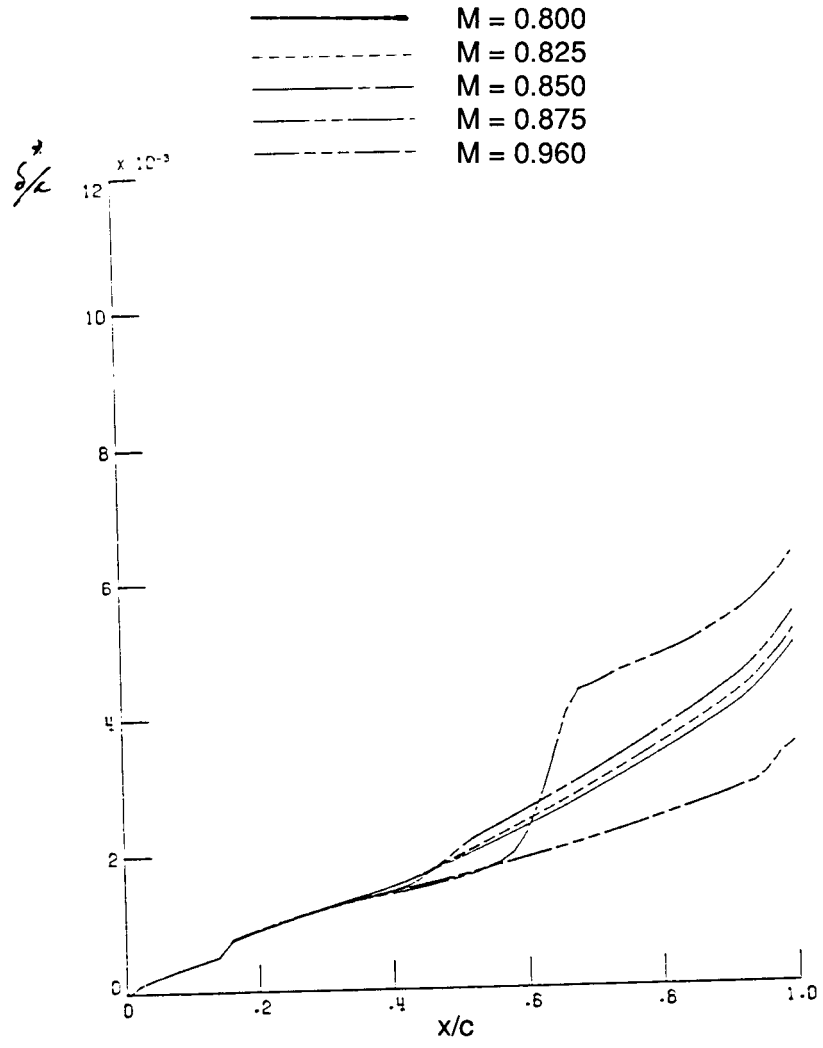

Unsteady pressure distributions are plotted for the NACA 64A006 airfoil with an oscillating flap for M = 0.850 and k = 0.242. The calculated mean pressures are similar to the steady pressure distributions for this Mach number. The effect of the viscous boundary layer can be seen in the results for the upper surface pressure distribution in the lower left hand side of the figure. The viscous unsteady pressure distributions agree very well with the experimental results, especially in the vicinity of the shock where the inviscid calculation shows the largest discrepancy. The interacting viscous boundary layer gives a substantial improvement over inviscid calculations in predicting the unsteady pressure distributions for this airfoil.

UNSTEADY PRESSURE DISTRIBUTION FOR NACA 64A006 AIRFOIL
M = 0.850 K = 0.242

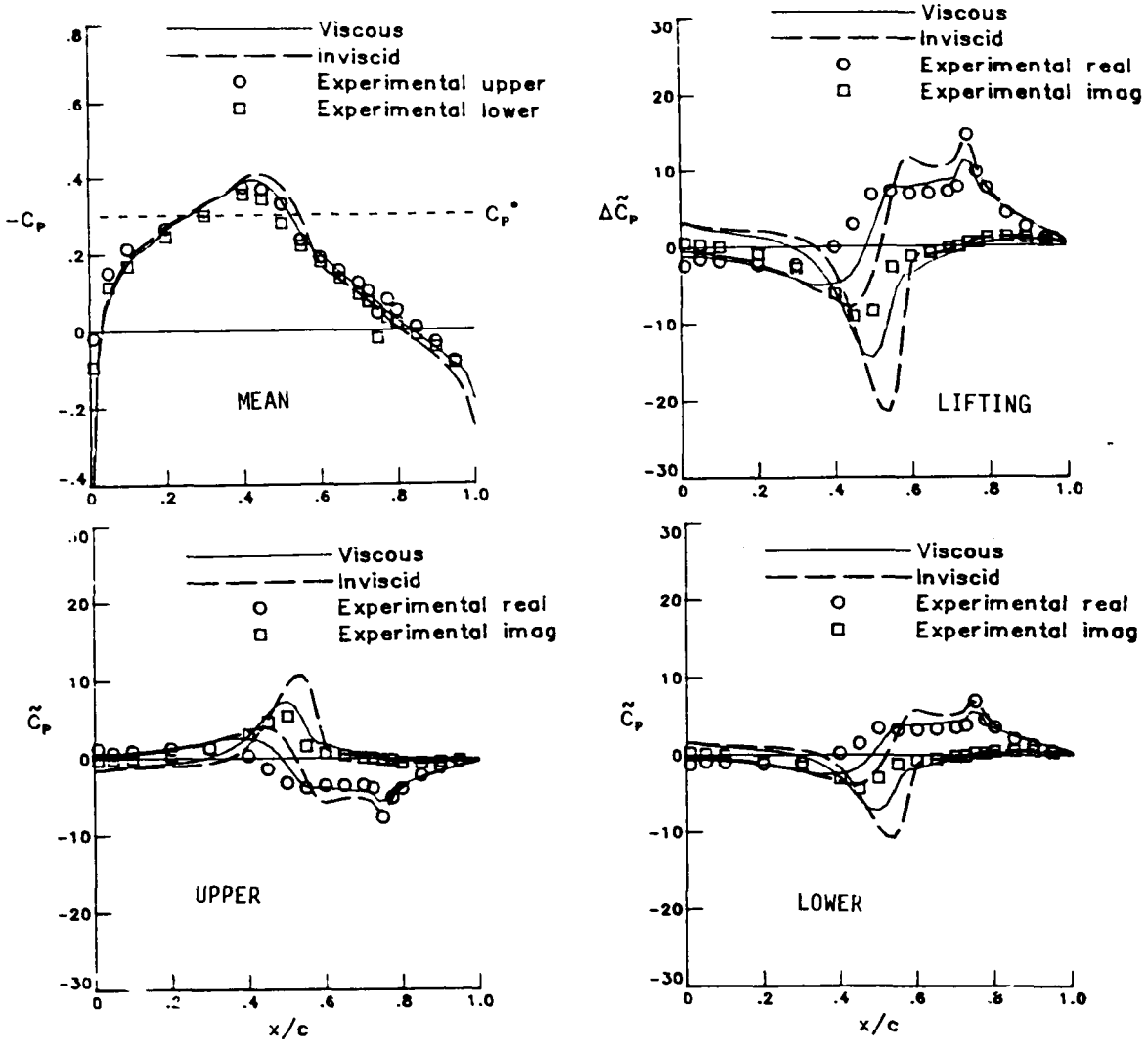

This figure shows plots of the unsteady lift as a function of mach number for the NACA 64A006 airfoil for a reduced frequency of 0.060. The results indicate that the viscous boundary layer corrects up to 25% of the differences between the inviscid results and the experiments for the lower values of Mach number. The linear theory results, also shown on the figure, are competitive with the CFD calculations for predicting the unsteady lift for most of the cases investigated for this airfoil.

COMPARISON OF UNSTEADY LIFT FOR NACA 64A006 AIRFOIL K = 0.060

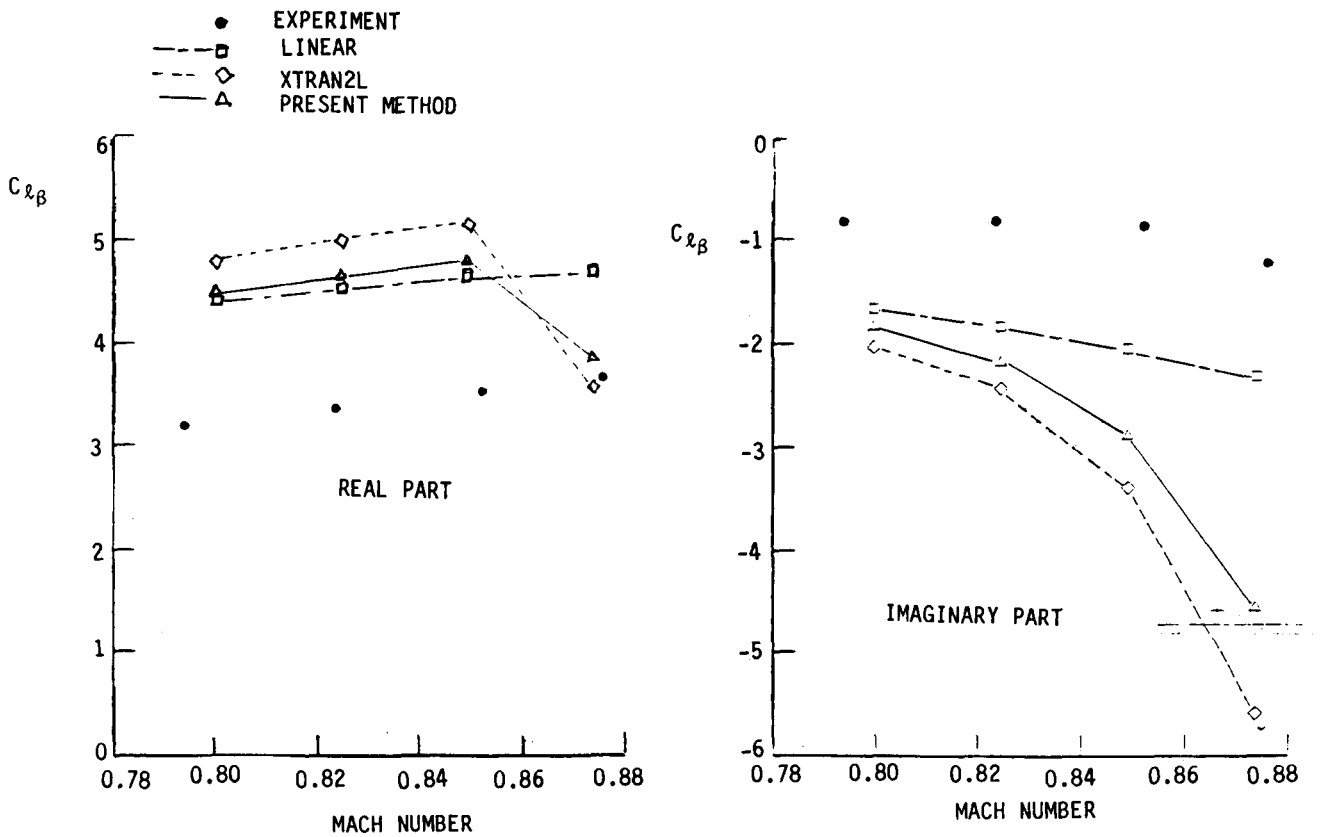

The steady pressure distributions for the MBB-A3 supercritical airfoil at the supercritical design point (M = 0.765, α_o = 1.5°) are plotted in this figure. The calculated cases are for the actual experimental values of Mach number and angle of attack rather than values adjusted to match flow conditions in the wind tunnel as is frequently done in comparison with this particular data. The experiment shows supercritical flow without a discernable shock wave typical of flow at the design point. The region of supercritical flow terminates at about x/c = 0.53. The viscous calculation indicates a moderate strength shock wave at nearly the same location. Away from the shock, agreement between the viscous calculation and the experiment is very good, although some discrepancies are noted near the leading edge on the lower surface. For this case, the inclusion of viscous effects yields a significant improvement in the calculation of the steady pressure distribution.

STEADY PRESSURE DISTRIBUTION FOR MBB-A3 AIRFOIL

M = 0.765 α_o = 1.5°

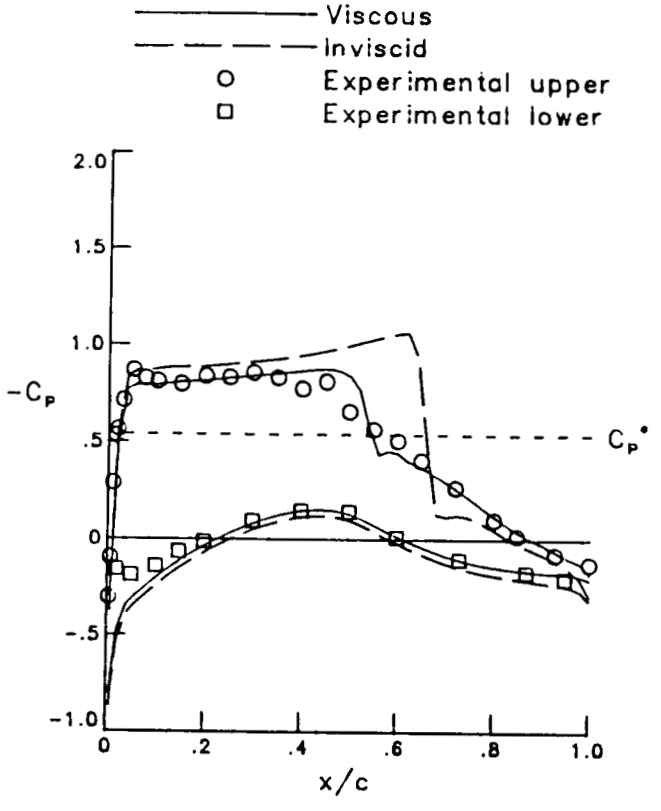

Steady pressure distributions for the NACA 64A010A (Ames) airfoil at M = 0.796 and $\alpha_o = 0^o$ have been calculated with the inviscid code, the viscous interaction theory, and non-isentropic corrections to the viscous interaction results. As the figure shows, the viscous calculation agrees better with the experimental results in so far as shock location and strength is concerned. The non-isentropic corrections move the shock position downstream about 1% chord and increase the shock strength slightly. In general however, differences between the experiment and all three calculated results are small.

STEADY PRESSURE DISTRIBUTION FOR NACA 64A010 AIRFOIL WITH NON-ISENTROPIC CORRECTIONS
M = 0.796

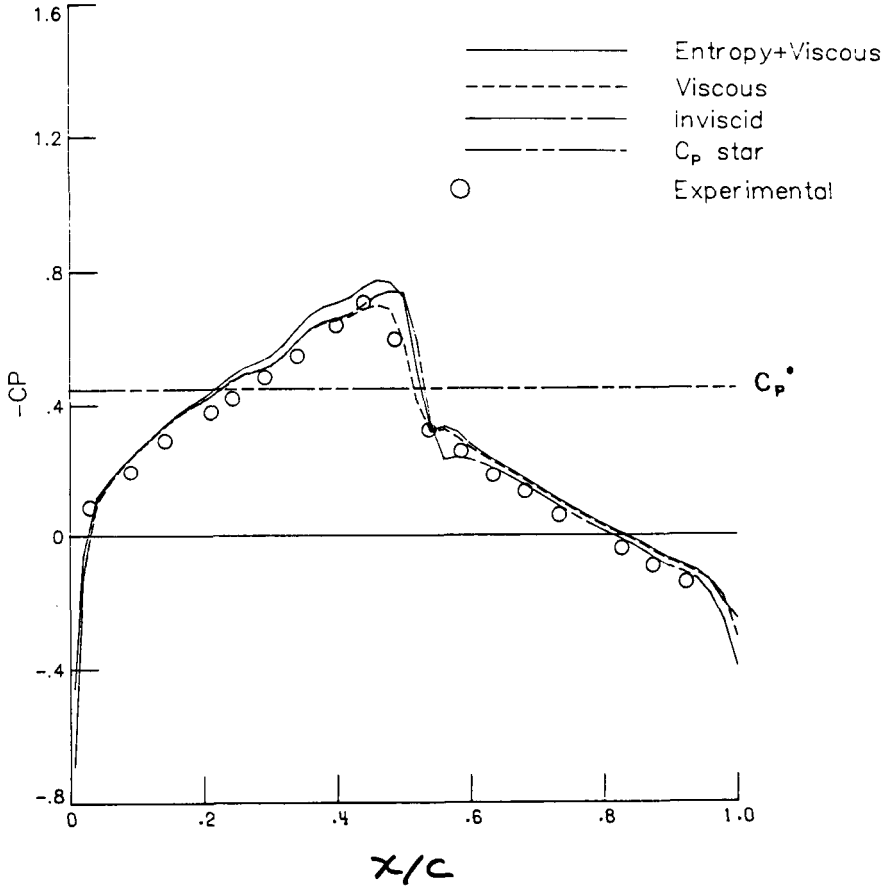

This figure shows plots of the unsteady pressure distributions for the NACA 64A010A (Ames) airfoil oscillating in pitch at M = 0.796 and k = 0.025. In contrast to the small effect the non-isentropic corrections have on the steady pressure distributions, these corrections to the viscous interaction theory give substantially better agreement with the unsteady experimental results. In the vicinity of the shock wave, the modified theory matches the experimental points very well, whereas the inviscid calculation is quite different. The significant improvement of calculated unsteady pressure distributions for this case due to the inclusion of non-isentropic and viscous effects is particularly interesting because the shock wave has only moderate strength.

UNSTEADY PRESSURE DISTRIBUTION WITH NON-ISENTROPIC CORRECTIONS FOR NACA 64A010 AIRFOIL

M = 0.796 K = 0.025

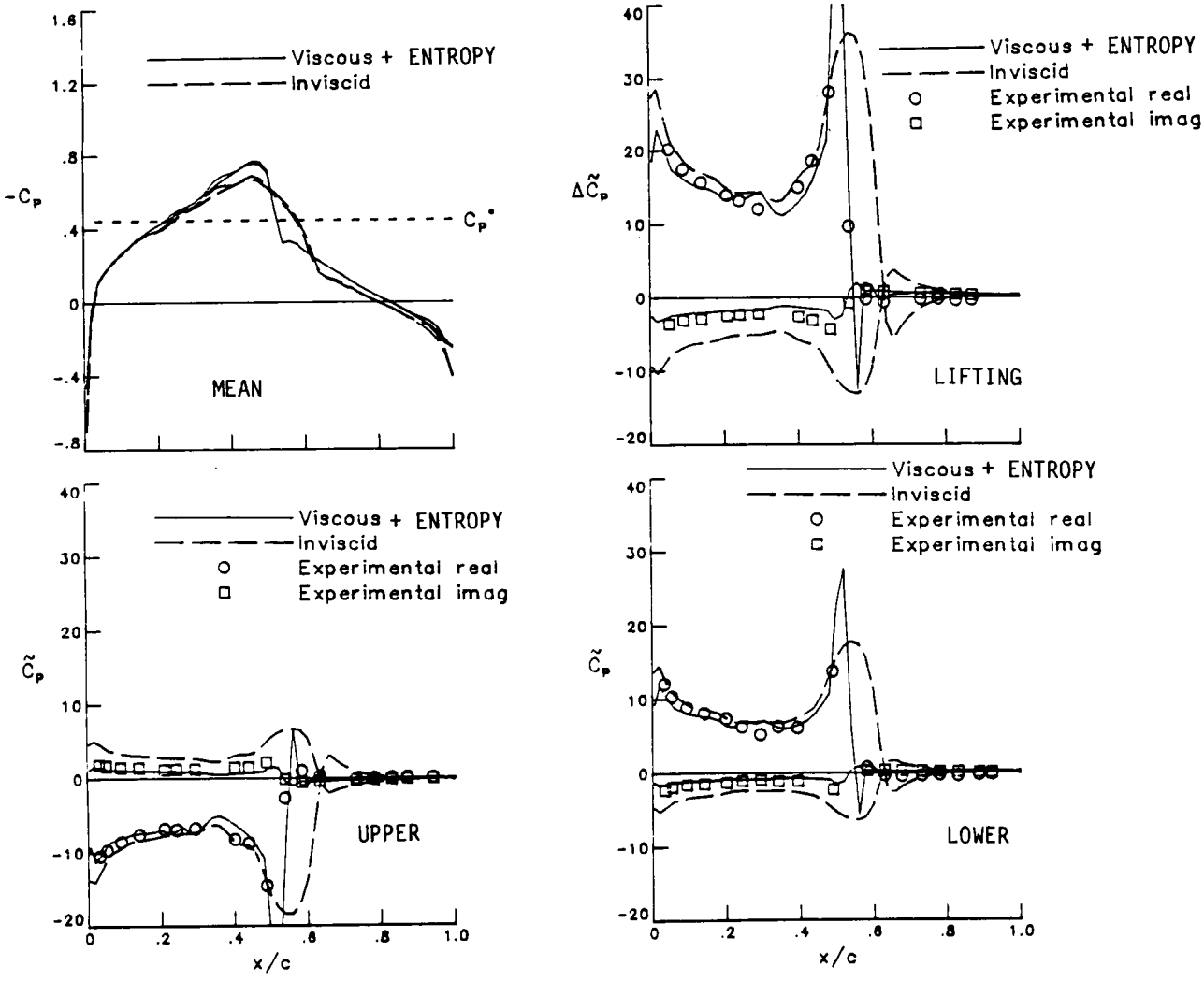

This figure presents comparisons of unsteady lift for calculated and experimental results for the NACA 64A010A (Ames) airfoil oscillating in pitch. The non-isentropic and viscous corrections give substantial improvements in the calculated values for low values of reduced frequency. This is especially evident in the imaginary part of the unsteady lift. Neither the inviscid nor viscous calculations predict the upward trend of the experimental results for low values of reduced frequency. The non-isentropic and viscous calculations show this low frequency upward trend very well, although some discrepancies are evident in the mid-frequency range. This significant improvement in lift predictions for low frequency cases re-emphasizes the importance of non-isentropic corrections even when the flow field does not exhibit strong shock waves.

COMPARISON OF UNSTEADY LIFT WITH NON-ISENTROPIC CORRECTIONS FOR NACA 64A010 AIRFOIL
M = 0.796

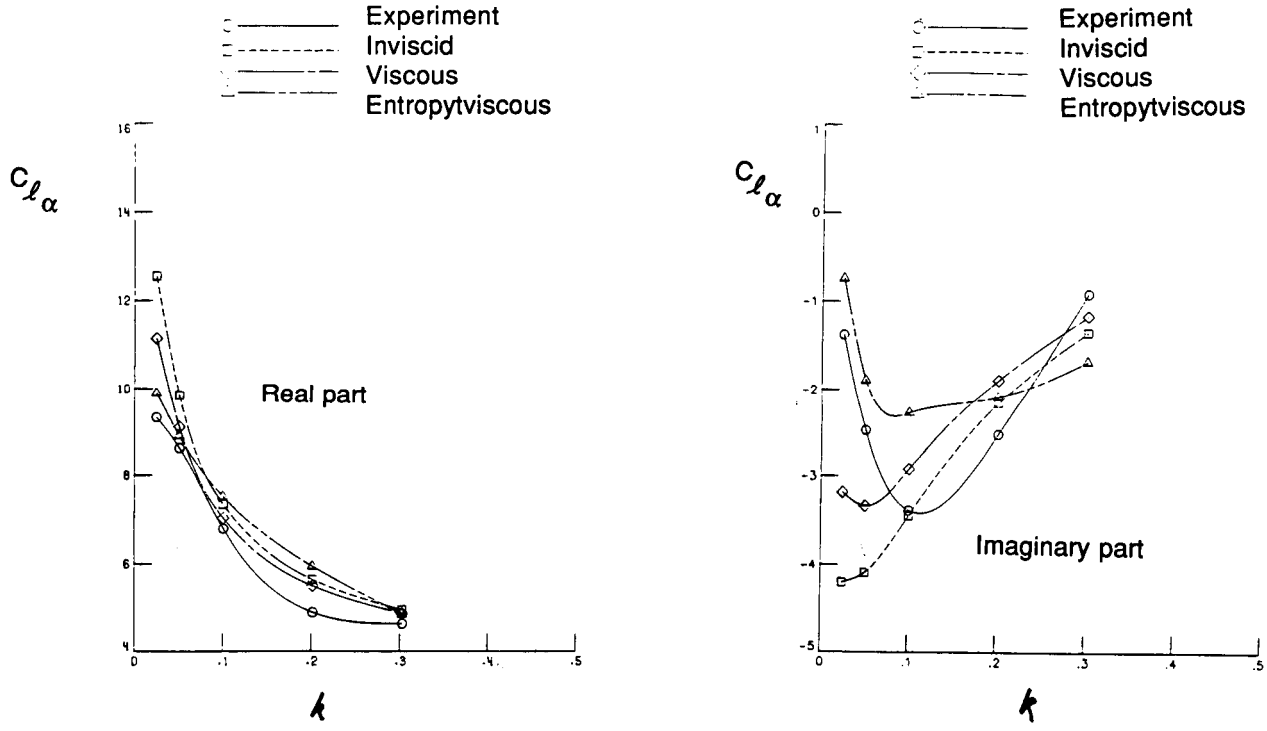

The inverse boundary-layer code has been used to calculate several test cases in which the flow is separated, or close to separation, in order to demonstrate the capabilities of the method. This figure shows plots of the steady pressure distributions for the NLR 7301 airfoil at M = 0.70 and α_o = 3°. Note the mean angle of attack is the actual experimental angle of 3° and not the corrected value of 2° which is specified in the AGARD conditions for this case. As the figure shows, the inverse boundary-layer code predicts a pressure distribution which agrees reasonably well with the experiment for this very difficult case. The calculated shock wave is about 5% chord upstream of the experiment and slightly weaker. The calculation also indicates a small region of separation at the trailing edge whereas the experimental pressures show no evidence of trailing edge separation.

STEADY PRESSURE DISTRIBUTION CALCULATED WITH INVERSE BL CODE FOR NLR 7301 AIRFOIL

M = 0.70 α_o = 3°

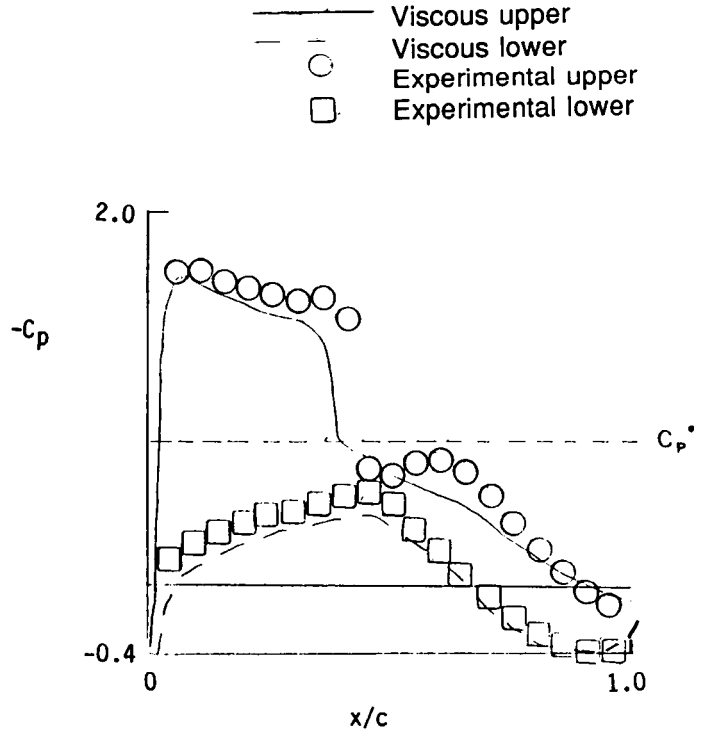

This figure shows unsteady pressure distributions for the NACA 0012 airfoil oscillating in pitch at M = 0.599. The mean angle of attack is 4.86° and the reduced frequency is k = 0.081. For the viscous calculation with the inverse boundary-layer method, transition is specified to be at 20% chord. The mean pressure distributions show the calculated results underestimating the suction peak near the leading edge with the inviscid calculation being slightly closer to the experiment in this region. Over the rest of the airfoil, both viscous and inviscid calculations agree well with the experiment. The unsteady pressure distributions on the airfoil upper surface are well predicted by both viscous and inviscid calculations with the viscous shock location slightly upstream of the inviscid result. The viscous calculation indicates that the flow is very close to separation near the maximum angle of attack of 7.3°. In fact, as shown in the next figure, a small change in the specified position of transition for the viscous calculation can result in flow separation during part of the oscillation cycle.

UNSTEADY PRESSURE DISTRIBUTION CALCULATED WITH INVERSE BL CODE FOR NACA 0012 AIRFOIL

M = 0.599 α_0 = 4.86° α_1 = 2.44° K = 0.081

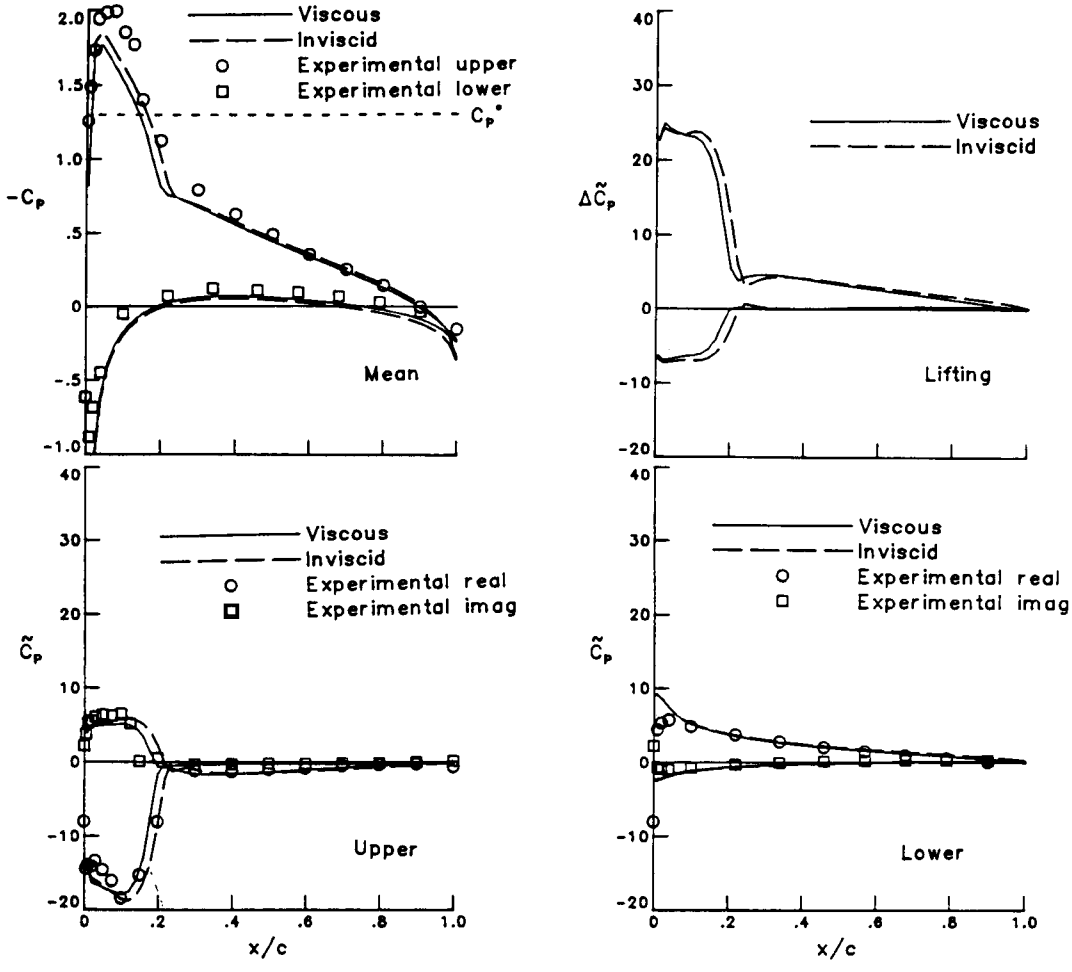

This figure shows plots of the unsteady lift and moment coefficients for the NACA 0012 airfoil as calculated by the inverse boundary-layer method with transition specified at 10% chord. With transition at this location, which is upstream of the shock wave, the boundary-layer displacement thickness increases significantly across the shock wave. This increased displacement thickness causes the flow to separate just after maximum lift. The lift coefficient plotted in the figure clearly shows the sudden decrease in lift associated with flow separation and the corresponding increase in lift upon reattachment. After the flow reattaches, the lift coefficient continues to vary smoothly throughout the rest of the cycle. The inverse boundary-layer method successfully captures this flow separation and reattachment without difficulty.

UNSTEADY LIFT CALCULATED WITH INVERSE BL CODE FOR NACA 0012 AIRFOIL

M = 0.599 α_0 = 4.86° α_1 = 2.44° K = 0.81

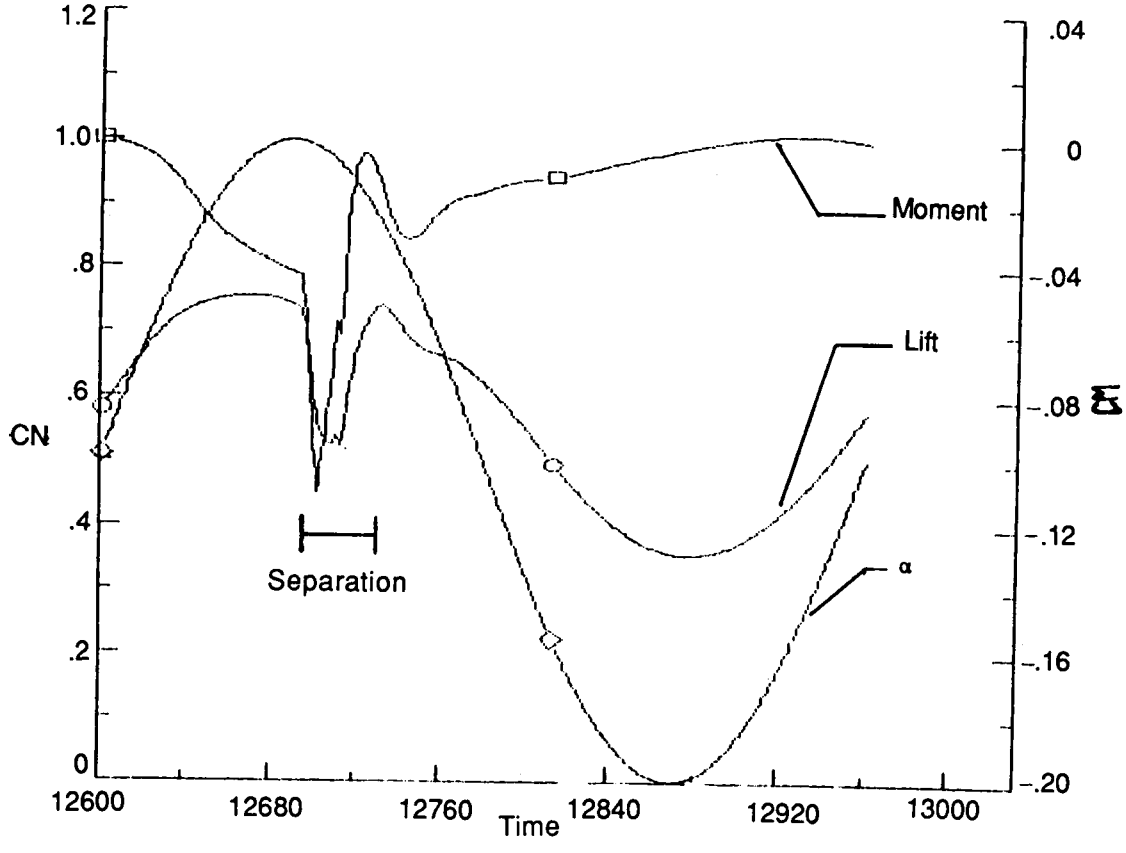

This paper has presented comparisons of calculated and experimental results for unsteady transonic flows over airfoils. The calculations include results obtained from a viscous-inviscid interaction method based upon the 2-D XTRAN2L inviscid transonic computer code. Non-isentropic corrections have been included in some cases. The viscous boundary-layer equations have been solved in the direct mode for attached flow and an inverse mode for separated flow. The results have demonstrated that pressures and forces calculated by the viscous-inviscid interaction method compare well with experimental results for steady and unsteady attached flows. The non-isentropic corrections with the viscous interaction method provided improved comparisons with experiments for unsteady low frequency oscillations in cases involving moderate strength shock waves. Initial applications of the inverse boundary-layer method have demonstrated that this method can calculate unsteady flow fields involving flow separation and reattachment. The results indicate that the viscous-inviscid interaction method can provide accurate predictions of viscous effects in unsteady transonic flow fields.

CONCLUSIONS

- PRESSURES AND FORCES CALCULATED BY VISCOUS-INVISCID INTERACTION COMPARE WELL WITH EXPERIMENTS FOR STEADY AND UNSTEADY ATTACHED FLOW

- NON-ISENTROPIC CORRECTIONS WITH VISCOUS INTERACTION YIELD IMPROVED COMPARISONS WITH EXPERIMENTS FOR UNSTEADY LOW FREQUENCY OSCILLATIONS

- INVERSE BOUNDARY LAYER METHOD HAS POTENTIAL FOR CALCULATING UNSTEADY FLOW SEPARATION AND REATTACHMENT

REFERENCES

1. Whitlow, Woodrow, Jr.: XTRAN2L: A Program for Solving the General-Frequency Unsteady Transonic Small Disturbance Equation. NASA TM 85723, November 1983.

2. Rizzetta, Donald P.: Procedures for the Computation of Unsteady Transonic Flows Including Viscous Effects. NASA CR 166249, January 1982.

3. Howlett, James T.: Efficient Self-Consistent Viscous-Inviscid Solutions for Unsteady Transonic Flow. AIAA Paper No. 85-0482, 23rd Aerospace Sciences Meeting, Reno, Nevada, January 14-17, 1985.

4. Fuglsang, Dennis F; and Williams, Marc H.: Non-Isentropic Unsteady Transonic Small Disturbance Theory. AIAA Paper No. 85-0600, AIAA/ASME/ASCE/AHS 26th Structures, Structural Dynamics and Materials Conference, Orlando, Florida, April 1985.

5. Vatsa, V. N.; and Carter, J. E.: Development of an Integral Boundary-Layer Technique for Separated Turbulent Flow. United Technologies Research Center, Report No. UTRC 81-28, April 1981.

6. Carter, James E.: A New Boundary-Layer Inviscid Iteration Technique for Separated Flow. AIAA Computational Fluid Dynamics Conference, Williamsburg, VA, July 23-25, 1979.